Polydeoxyribonucleotide and Shock Wave Therapy Sequence Efficacy in Regenerating Immobilized Rabbit Calf Muscles

Yoon-Jin Lee , Yong Suk Moon , Dong Rak Kwon * , Sung Cheol Cho , Eun-Ho Kim

Posted Date: 26 July 2023

doi: 10.20944/preprints202307.1799.v1

Keywords: Muscle atrophy; Polydeoxyribonucleotides; Extracorporeal shock wave therapy; Muscle regeneration; Rabbit models

Article

Polydeoxyribonucleotide and Shock Wave Therapy Sequence Efficacy in Regenerating Immobilized Rabbit Calf Muscles

Yoon-Jin Lee [3†], Yong Suk Moon [2†], Dong Rak Kwon, [1*], Sung Cheol Cho [1] and EunHo Kim [4]

[1] Department of Rehabilitation Medicine, Catholic University of Daegu School of Medicine, Daegu, South Korea
[2] Department of Anatomy, Catholic University of Daegu School of Medicine, Daegu, South Korea
[3] Department of Biochemistry, College of Medicine, Soonchunhyang University, Cheonan, South Korea
[4] Department of Biomedical Engineering & Radiology, School of Medicine, Daegu Catholic University, Daegu 42472 Korea
* Correspondence: Dong Rak Kwon, MD, PhD, Department of Rehabilitation Medicine, Catholic University of Daegu School of Medicine, 33 Duryugongwon-ro 17-gil, Nam-Gu, Daegu, 42472, Korea, Telephone: 82-53-650-4878, Fax: 82-53-622-4687, E-mail: coolkwon@cu.ac.kr or dongrakkwon@hotmail.com
† Y.J.L. and Y.S.M. contributed equally to this work.

Abstract: The main purpose of the study is to investigate the combined effects of polydeoxyribonucleotide (PDRN) and extracorporeal shock wave therapy (ESWT) sequences on the regenerative processes in atrophied animal muscles. Thirty male New Zealand rabbits, aged 12 weeks, were divided into five groups: normal saline, PDRN, ESWT, PDRN injection before ESWT, and PDRN injection after ESWT. Following 2 weeks of cast immobilization, the respective treatments were administered to the atrophied calf muscles. Radial ESWT was performed twice weekly. The evaluation included measurements of calf circumference, tibial nerve compound muscle action potential (CMAP), and gastrocnemius (GCM) muscle thickness after 2 weeks of treatment. Histological and immunohistochemical staining, as well as Western blot analysis, were conducted 2 weeks post-treatment. Staining intensity and extent were assessed using semi-quantitative scores. Groups 4 and 5 demonstrated significantly greater calf muscle circumference, GCM muscle thickness, tibial nerve CMAP, and GCM muscle fiber cross-sectional area (types I, II, and total) than in the remaining three groups ($p < 0.05$), while they did not did not differ significantly in these parameters. Groups 2 and 3 showed the higher values for all the observations compared to group 1 ($p < 0.05$). Group 4 had the greatest ratio of vascular endothelial growth factor (VEGF) to platelet endothelial cell adhesion molecule-1 (PECAM-1) in the gastrocnemius muscle fibers than in the other four groups ($p < 0.05$). Western blot analysis revealed significantly higher expression of angiogenesis cytokines in groups 4 and 5 than in the remaining ($p < 0.05$). The combination of ESWT and PDRN injection demonstrated superior regenerative efficacy for atrophied calf muscle tissue in rabbit models than these techniques alone or saline. Particularly, administering ESWT after PDRN injection yielded the most favorable outcomes in specific parameters.

Keywords: muscle atrophy; polydeoxyribonucleotides; extracorporeal shock wave therapy; muscle regeneration; rabbit models

1. Introduction

Muscle atrophy, characterized by a decrease in muscle volume, can result from various factors such as malnutrition, nerve dysfunction, lack of physical activity. In a former study, it was discovered that there is a regression in the capillary network, a vital component responsible for delivering nutrients and immune cells to facilitate the healing and regeneration process of atrophied muscles [1]. Immobilization, which is often necessary during the recovery period from injuries or orthopedic

 doi:10.20944/preprints202307.1799.v1

surgeries, can lead to detrimental effects on muscle health, including reduced number of myofibrillar proteins, impaired metabolism, altered vascularization, and increased fat tissue within the muscles [2,3]. Maintaining muscle mass and function during periods of immobilization is crucial for optimal recovery and rehabilitation.

Muscle atrophy, characterized by a decline in muscle volume, can be attributed to various factors such as malnutrition, nerve dysfunction, physical inactivity, and immobilization. A previous study has highlighted the regression of the capillary network, a vital component responsible for facilitating the healing and regeneration process of atrophied muscles [1]. Immobilization, commonly required during the recovery phase following injuries or orthopedic surgeries, can have adverse effects on muscle health, including diminished myofibrillar proteins, impaired metabolic enzyme function, altered vascular and neural supply, and fat substitution within the muscles [2,3]. Preserving muscle mass and function during immobilization is of utmost importance for facilitating optimal recovery and rehabilitation outcomes. PDRN is a compound comprised of polymer chains of deoxyribonucleotides. It regulates the expression of cytokines, resulting in a decrease of pro-inflammatory cytokines, promoting tumor necrosis, and an increase in anti-inflammatory like interleukin-10 [4,5]. Additionally, PDRN has demonstrated the ability to stimulate the production and release of VEGF by augmenting the effects of adenosine on A2A receptors [6,7]. This mechanism plays a vital role in promoting angiogenesis and collagen synthesis, which are crucial for tissue healing and regeneration.

ESWT is a therapeutic modality that utilizes acoustic waves generated outside the body to target specific anatomical regions. Previous studies have provided evidence of the effectiveness of ESWT in reducing pain caused by peripheral nerve injuries and promoting revascularization [8]. It has also been shown to stimulate axon regeneration and provide pain relief [9]. ESWT has gained widespread application in the management of various musculoskeletal conditions, including calcific tendinopathy, lateral epicondylitis, spasticity, and plantar fasciitis [10–13]. A systematic review even suggested that ESWT is comparable in effectiveness to botulinum toxin for the treatment of post-stroke spastic aggravations [13]. Nonetheless, the available evidence regarding the role of ESWT in muscle regeneration following injuries or atrophy remains limited.

In a rat model, studies have demonstrated the beneficial effects of ESWT on sciatic nerve function and prevention of denervation atrophy. This was evidenced by improved sciatic functional index scores compared to control groups [14]. Additionally, ESWT has been shown to stimulate the response mechanisms in skeletal muscle tissue following injury in another rat model [15]. The underlying mechanisms behind these effects are believed to involve mechanotransduction and the upregulation of various growth factors, including insulin-like growth factor (IGF), fibroblast growth factor (FGF), and VEGF.

In a previous study, our aim was to investigate the effects of combining ESWT with PDRN injection in full-thickness rotator cuff tendon tear rabbit models [16]. The results of our study demonstrated that this combined approach yielded superior outcomes in terms of revascularization, cell proliferation, and fast walking time compared to ESWT alone, PDRN injection alone, or normal saline injection. Notably, applying ESWT prior to PDRN injection further improved the outcomes. However, it is important to note that no studies have been performed thus far to study the effects of different sequences of combination of ESWT with PDRN injection on atrophied calf muscles in rabbits immobilized in a cast.

The main purpose of the study is to explore the combined effects of different sequences of extracorporeal shockwave therapy (ESWT) and polydeoxyribonucleotide (PDRN) injection on atrophied calf muscles in rabbit models subjected to cast immobilization. By elucidating the optimal treatment sequence, our aim is to enhance our understanding of the synergistic effects of these interventions and their potential for promoting muscle regeneration. This article complies with the ARRIVE reporting checklist.

2. Methods

2.1. Animal models:

Preprints (www.preprints.org) | NOT PEER-REVIEWED | Posted: 26 July 2023 doi:10.20944/preprints202307.1799.v1

Approval for this study was obtained from the Institutional Animal Care and Use Committee (IACUC) of the Catholic University of Daegu School of Medicine (IRB no.: DCIAFCR-210503-01-Y). Thirty male New Zealand white rabbits, aged 12 weeks, and weighing a mean of 3.3 kg, were utilized for the research. The rabbits were individually placed in steel cages under monitored environmental conditions, including a temperature of 23°C ± 2°C and humidity of 45% ± 10%, while tap water and commercial rabbit diet were provided for nutrition.

Random assignment of the animals into five groups, with six rabbits in each group, was carried out using a random grouping program by assigning numbers from one to thirty to the rabbits. The groups were as follows: Group 1 (G1-Control) received a normal saline injection (0.7 ml); Group 2 (G2-PDRN) received an injection of polydeoxyribonucleotide (PDRN) (0.7 ml); Group 3 (G3-ESWT) underwent extracorporeal shockwave therapy (ESWT); Group 4 (G4-PDRN+ESWT) received an injection of PDRN (0.7 ml) followed by ESWT; and Group 5 (G5-ESWT+PDRN) underwent ESWT followed by an injection of PDRN (0.7 ml) (Figure 1).

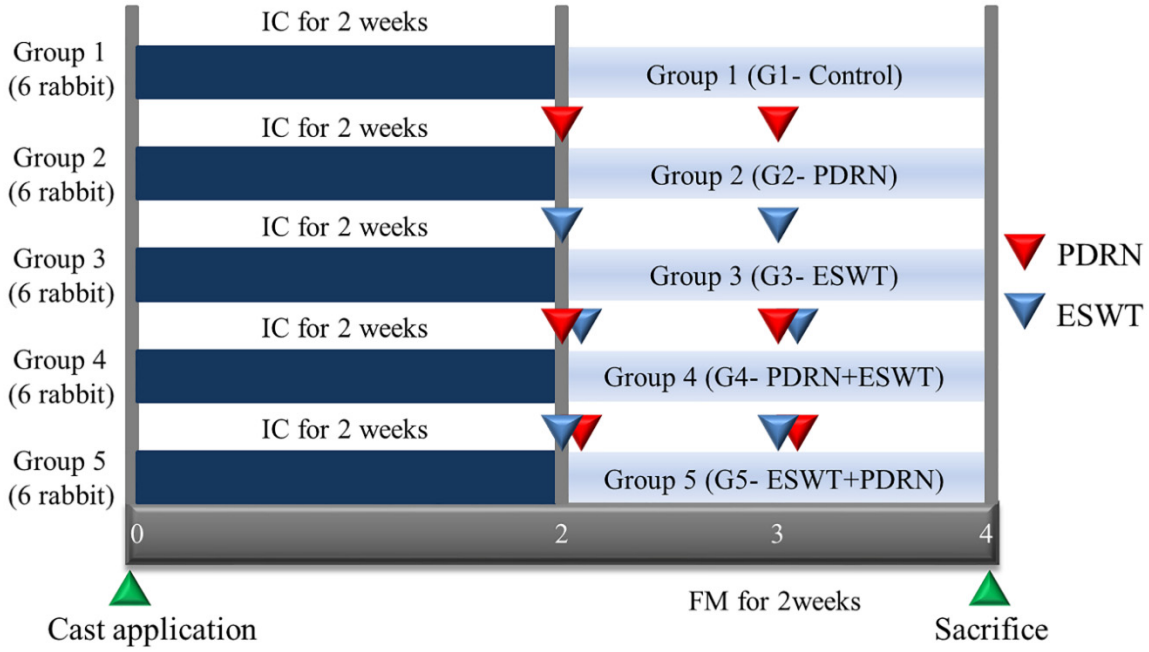

Figure 1. Timeline of the study. A total of 30 rabbits were randomly allocated to 5 groups. G1-Control: IC for 2 weeks and 0.7 mL of normal saline injection for 2 weeks after CR; G2-PDRN: IC for 2 weeks and 0.7 mL of PDRN injection for 2 weeks after CR; G3-ESWT: IC for 2 weeks and ESWT after CR; G4-PDRN+ESWT: IC for 2 weeks and 0.7 mL of PDRN injection and ESWT for 2 weeks after CR; G5-ESWT+PDRN: IC for 2 weeks and 0.7 mL of ESWT injection and PDRN for 2 weeks after CR. IC: immobilized by cast; NS: normal saline; PDRN: polydeoxyribonucleotide; ESWT: extracorporeal shock wave therapy; FM: free movement; CR: cast removal.

2.2. Immobilization by cast:

The right lower limbs of rabbits were immobilized with a cast for a duration of 2 weeks. The immobilization process involved extending the right knees and ankles by utilizing a splint composed of an adhesive elastic bandage and PVC material (Tensoplast®; Smith & Nephew Medical, London, UK). This immobilization technique was conducted following the procedure outlined in a prior study [17].

2.3. Injection:

Injection was performed with Zoletil® 50 (15 mg/kg, Virbac Korea, Seoul, Korea) and xylazine (5 mg/kg, Rompun®; Bayer Co., Seoul, Korea) administered intramuscularly. Ultrasound guidance was employed, utilizing a 5-13-MHz multifrequency linear transducer (Antares; Siemens Healthcare,

Preprints (www.preprints.org) | NOT PEER-REVIEWED | Posted: 26 July 2023 doi:10.20944/preprints202307.1799.v1

Erlangen, Germany). Injections of normal saline or PDRN (0.7 ml each) were administered at both sides of the GCM muscle with the aid of ultrasound imaging (Figures 2A, 2B). For this purpose, commercial PDRN (Rejuvenex Inj., Polydeoxyribonucleotide sodium, 5.625 mg/3 ml, Pharma Research Product, South Korea) was utilized. Each injection of 0.35 ml was performed from two sides horizontally, guided by a central reference point. The central reference point was determined as the midpoint between the malleoli of both ankles and that between the femoral epicondyles, with a horizontal line perpendicular to the intersection of the longitudinal line. The injections were carried out repeatedly at the same sites one week after.

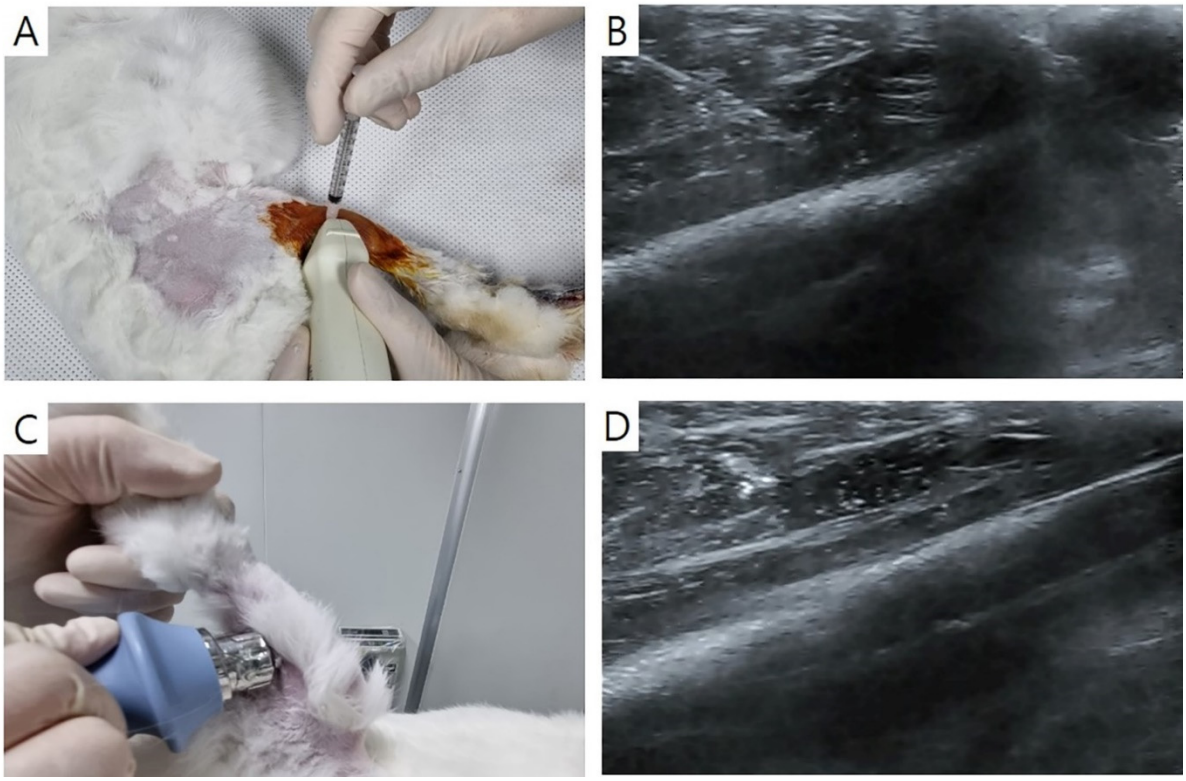

Figure 2. Longitudinal ultrasound image showing PDRN injection at 0.7 mL (A) under ultrasound guidance (needle, red arrows) in the right gastrocnemius muscles of a rabbit (B). ESWT (C) was then performed under ultrasonic guidance to the region of interest, focusing on the PDRN injection area (D). GCM: gastrocnemius; PDRN: polydeoxyribonucleotide; ESWT: extracorporeal shock wave therapy.

2.4. ESWT:

ESWT was performed using a radial-type machine (BTL-5000; BTL, Columbia, SC, USA). Pressure pulses were applied to both sides of the GCM muscle. In the case of Group 4, ESWT was administered immediately following PDRN injection (Figures 2C, 2D). Each injection site received a total of 750 shocks, resulting in a cumulative total of 1500 shocks (two sites; energy density = 0.1 mJ/mm2; frequency = 3 pulses/s). ESWT was performed repeatedly at the same site one week after.

2.5. Clinical procedure:

The measurements of all study parameters were performed by a physician who had extensive experience in ultrasound (20 years) and electrophysiology (25 years). The assessment was conducted in a blinded manner to minimize bias. Before euthanasia, a motor nerve conduction was evaluated in order to detect the amplitude of the CMAP on tibial nerve. The active and reference electrodes were placed at the midpoint of GCM muscle and at the ankle, respectively. Electrical stimuli were conveyed to the tibial nerve in the popliteal fossa, and the highest CMAP was observed after 7-10 of them.

Preprints (www.preprints.org) | NOT PEER-REVIEWED | Posted: 26 July 2023 doi:10.20944/preprints202307.1799.v1

The measurements of calf were done using tape with the knee joints flexed at a 90° angle and the ankle in a relaxed position. Real-time B-mode ultrasound was utilized to assess the dimensions of GCM muscle to the deepest layers of fascia (Figure 3). Longitudinal ultrasound images of the GCM were received at the injection sites on both surfaces of the muscle.

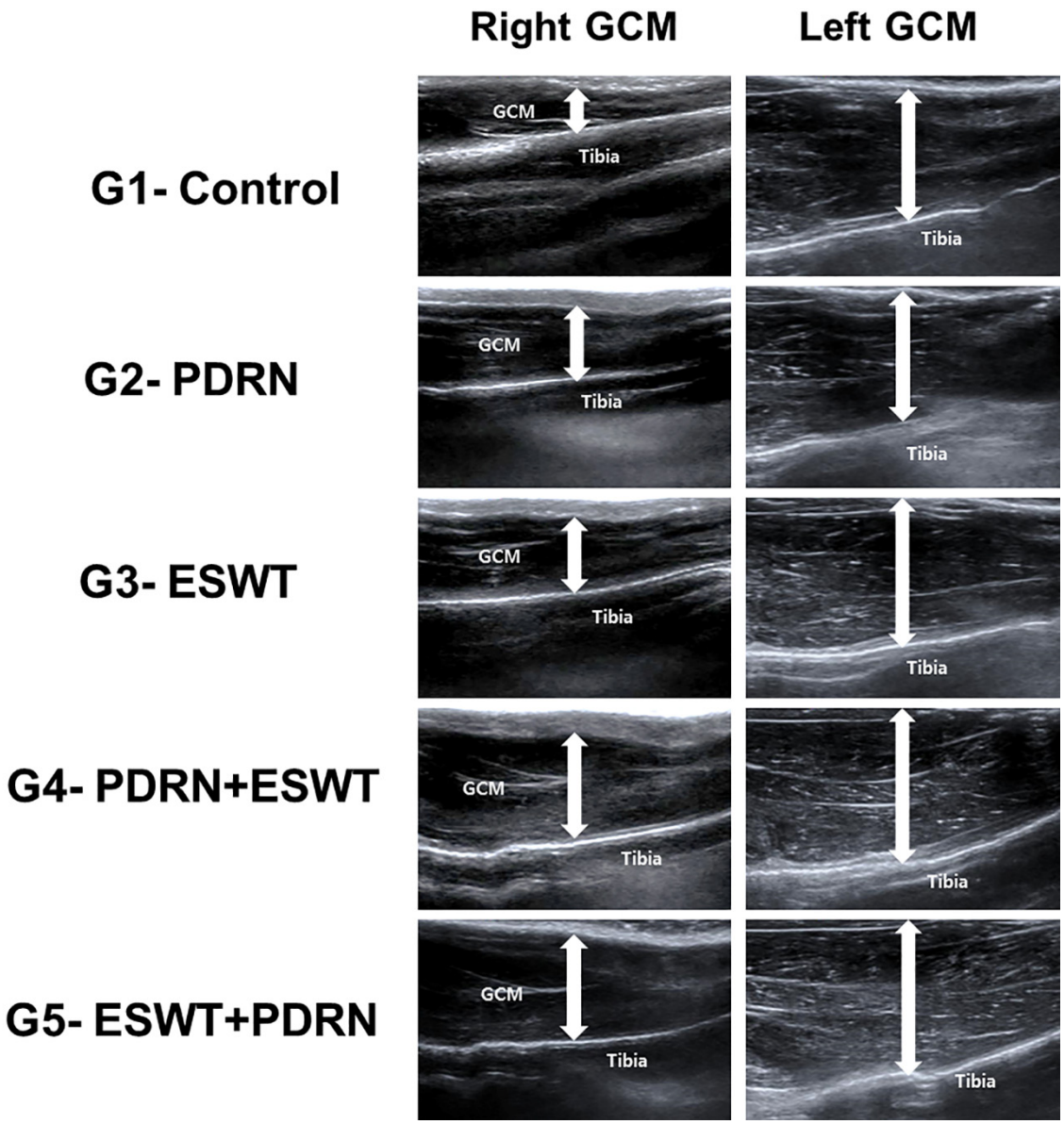

Figure 3. GCM muscle thickness was measured via ultrasound. Thickness was measured as the distance from the superficial aponeurosis to the GCM muscle deep aponeurosis (up-down arrows). Representative longitudinal sonograms of the right and left GCM muscles. The atrophic change of the right GCM muscle was less pronounced in the rabbits in the G4-PDRN+ESWT and G5-ESWT+PDRN groups than that in the other three groups. NS: normal saline; PDRN: polydeoxyribonucleotide; ESWT: extracorporeal shock wave therapy; GCM: gastrocnemius.

To evaluate atrophic changes, the CMAP amplitude, GCM thickness, and calf circumference were calculated with the formula: ([left side - right side]/left side × 100). The results were presented as the difference in the percentages of atrophic changes on the both sides.

2.6. Tissue preparation:

At 2 weeks after the removal of cast immobilization, all rabbits were euthanized under general anesthesia. All histological examinations were done from the blinded sample, and muscle samples

 doi:10.20944/preprints202307.1799.v1

were obtained from the right GCM. The lateral and medial GCM muscle fibers were isolated and stored in neutral-buffered formalin for one day. Subsequently, the specimens were embedded in paraffin (Paraplast; Oxford, St. Louis, MO, USA) and divided into 5-mm thick transverse sections for further analysis.

2.7. Immunohistochemical analysis:

Immunohistochemical analysis was carried out on the muscle sections to identify types I and II fibers using monoclonal anti-myosin antibodies (Sigma-Aldrich, St. Louis, MO, USA). Specific monoclonal antibodies targeting type I (skeletal, slow) and type II (skeletal, fast) fibers were utilized. Furthermore, the sections were subjected to immunostaining for angiogenic markers using a polyclonal anti-VEGF antibody (A-20; Santa Cruz Biotechnology) and an anti- PECAM-1 polyclonal antibody (M-20; Santa Cruz Biotechnology).

The paraffin-placed sections were rinsed with PBS, and to inhibit endogenous peroxidases, they were treated with 0.3% H2O2 in PBS for 30 minutes. Non-specific protein binding was prevented by further placement of them in PBS having 10% normal horse serum (Vector Laboratories, Burlingame, CA, USA) for 30 minutes. Then the respective primary antibodies (diluted at 1:200-1:500) at room temperature for 2 hours, were added, and three rinses with PBS were done. Subsequently, the appropriate secondary antibody (diluted at 1:100) were added. Biotinylated anti-mouse immunoglobulin G (IgG) (Vector Laboratories) was stored in the muscle sections for 1 hour at room temperature. Followed by three rinses with PBS, avidin-biotin-peroxidase complex (ABC, Vector Laboratories) was retained in the sections for 1 hour, and rinsing was done three times more. The peroxidase reaction was carried out with 0.05 M Tris-HCl (pH 7.6) having 0.01% H2O2 and 0.05% 3,3'-diaminobenzidine (DAB, Sigma-Aldrich). Hematoxylin was used for counterstaining, and the slides were mounted. The stained slides were examined using an Axiophot Photomicroscope (Carl Zeiss, Oberkochen, Germany) with an Axio-Cam MRc5 attachment (Carl Zeiss).

The histological examinations were blinded, Axiophot Photomicroscope (Carl Zeiss) was used. Five randomly selected fields were captured from each group for analysis. The morphometric analysis was done by software (AxioVision SE64; Carl Zeiss) that was used to evaluate the mean value of the cross-sectional area (CSA) of anti-myosin positive type I and II muscle fibers.

Photographs of 20 randomly selected fields were taken from each group and analyzed with the same software for counting the ratio of the number of VEGF- and PECAM-1-positive cells or nuclei per 1,000 muscle fibers, as well as the total number of muscle fibers per image.

2.8. Tissue Western blot:

Calf tissue samples were stored in radioimmunoprecipitation assay buffer (1× PBS, 1% NP-40, 0.5% sodium deoxycholate, 0.1% sodium dodecyl sulfate [SDS], 10 µg/mL of phenylmethanesulfonyl fluoride, and a protease inhibitor cocktail tablet) for 1 minute on ice. The homogenates were then centrifuged at 10,000 ×g for 10 minutes at 4°C, and then kept at -70°C for subsequent Western blot analysis. The protein concentration in the supernatants was determined using a BCA assay kit (Thermo Scientific Inc., Waltham, MA, USA) following the manufacturer's instructions.

For Western blot analysis, 40 µg of protein samples were divided by SDS-polyacrylamide gel electrophoresis using NuPAGE 4%–12% bis-Tris gels (Invitrogen, Waltham, MA, USA) and delivered to polyvinylidene difluoride (PVDF) membranes (GE Healthcare Life Sciences, Amersham, Bucks, Germany). The latter were then stored in casein blocking buffer (Sigma-Aldrich Corp., St. Louis, MI, USA), and the antibodies were added. After applying washing and PBS tween-20 buffers, the membranes were saturated for 1 hour with anti-mouse IgG (sc-2005; Santa Cruz Biotechnology)-HRP-linked species-specific whole antibody (diluted 1:5,000). Enhanced chemiluminescence revealed protein bands on membranes (Promega Corp., Madison, WI, USA), and an anti-β-actin antibody (A2228; Sigma-Aldrich Corp.) was added for loading control. The primary antibodies were against PCNA (sc-56; Santa Cruz Biotechnology), PECAM-1 (sc-376764; Santa Cruz Biotechnology), and VEGF (sc-7269; Santa Cruz Biotechnology). The relative density of the protein bands was quantitatively analyzed using TINA software (Version 2.10e).

Preprints (www.preprints.org) | NOT PEER-REVIEWED | Posted: 26 July 2023 doi:10.20944/preprints202307.1799.v1

2.9. Statistical analysis:

The data was analyzed using IBM Corp.'s Statistical Package for the Social Sciences version 22.0 for Windows. A significance level of 0.05 was used and the p-values less than 0.05 were considered statistically significant. To determine the appropriate sample size, a pilot study was conducted using the total muscle fiber CSA of the medial GCM as the primary endpoint. One rabbit from each group was included in the pilot study, and five randomly selected fields were evaluated in each group. Based on the effect size of 0.49 received from the pilot study, ANOVA analysis showed that 111 fields were required to attain the power of 95 %. Since four fields could be obtained from one rabbit, a total of 27 rabbits were initially considered. Accounting for a potential dropout rate of 10%, the final sample size was calculated to be 30 rabbits. Descriptive statistics, including means and standard errors, were calculated, and ANOVA was employed to make the comparisons among the four groups. When significant differences were observed, Tukey's test was performed for post hoc analysis, and 95% confidence intervals were calculated.

3. Results

The results showed significant differences in the imaging, electrophysiology, and clinical measurements between Group 1 (normal saline) and the other groups ($p < 0.05$, Table 1). The mean rates of atrophy in the right medial and lateral GCM muscle thickness, right calf circumference, and CMAP amplitude of the right tibial nerve were significantly lower in Groups 4 and 5 compared to the others ($p < 0.05$, Table 1). The values for the same parameters were also significantly lower in Groups 2 and 3 compared to Group 1 ($p < 0.05$, Table 1).

Immunohistochemical analysis revealed significant differences between Group 1 (normal saline) and the others ($p < 0.05$, Table 2, Figure 4). The mean CSA of type I medial and lateral GCM muscle fibers was significantly larger in Group 4 (1391.9 ± 23.6 μm2 and 1441.2 ± 25.9 μm2, respectively) and Group 5 (1137.9 ± 21.1 μm2 and 1095.1 ± 22.0 μm2) compared to the other three groups ($p < 0.05$, Table 2, Figure 4). Similarly, the mean CSA of type II muscle fibers was significantly larger in Group 4 (2458.0 ± 50.6 μm2 and 2460.4 ± 47.3 μm2, respectively) and Group 5 (2046.6 ± 33.8 μm2 and 1980.9 ± 27.6 μm2) compared to the other three groups ($p < 0.05$, Table 2, Figure 4). The mean CSA of both GCM muscle fibers (type I, II, and total) was significantly greater in Group 2 and Group 3 compared to Group 1 ($p < 0.05$, Table 2).

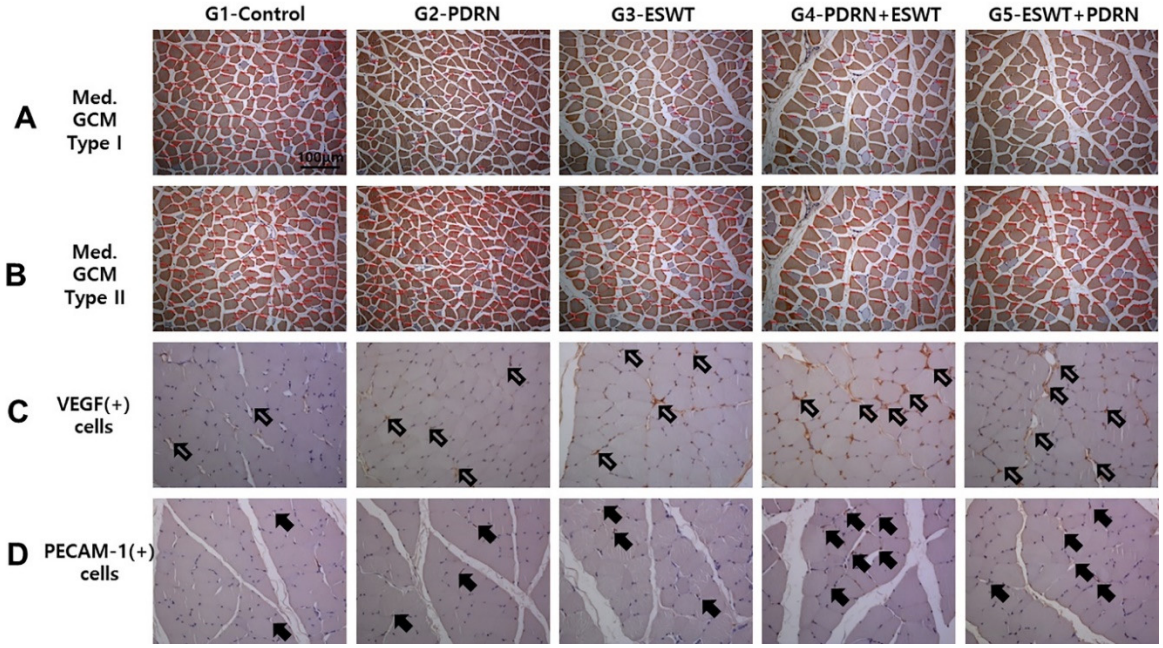

Figure 4. Representative immunohistochemical findings of the immobilized medial GCM muscles stained with monoclonal anti-myosin type I (A), type II (B), anti-VEGF (C), and anti-PECAM-1 (D) antibodies. The cross-sectional areas (red circles) of the medial head of GCM types I and II muscle

Preprints (www.preprints.org) | NOT PEER-REVIEWED | Posted: 26 July 2023 doi:10.20944/preprints202307.1799.v1

fibers were measured using an image morphometry program. The cross-sectional areas of muscle fibers were increased in the G2-PDRN, G3-ESWT, G4-PDRN+ESWT, and G5-ESWT+PDRN groups as compared with the G1-Control group. VEGF and PECAM-1-positive cell or nuclei (arrows) and the total number of muscle fibers within each image were counted. The VEGF and PECAM-1 ratio of the medial GCM muscle fibers in G4-PDRN+ESWT group were significantly higher than those in the other four groups. The scale bar is 50 μm. G1-Control: IC for 2 weeks and 0.7 mL of normal saline injection for 2 weeks after CR; G2-PDRN: IC for 2 weeks and 0.7 mL of PDRN injection for 2 weeks after CR; G3-ESWT: IC for 2 weeks and ESWT after CR; G4-PDRN+ESWT: IC for 2 weeks and 0.7 mL of PDRN injection and ESWT for 2 weeks after CR; G5-ESWT+PDRN: IC for 2 weeks and 0.7 mL of ESWT injection and PDRN for 2 weeks after CR. NS: normal saline; PDRN: polydeoxyribonucleotide; ESWT: extracorporeal shock wave therapy; GCM: gastrocnemius; VEGF: vascular endothelial growth factor; and PECAM-1: platelet endothelial cell adhesion molecule-1; IC: immobilization by cast.

Table 1. Comparison of the regenerative effect of clinical parameters among the five groups.

Atrophic changes (%)			
	Circumference of Rt. Calf (cm)	**CMAP on Rt. Tibial nerve (mV)**	**Rt. GCM muscle thickness (mm)**
G1-Control	24.1 ± 1.6	25.7 ± 2.0	23.6 ± 1.3
G2-PDRN	21.6 ± 4.0*	20.2 ± 5.0*	17.6 ± 3.1*
G3-ESWT	21.4 ± 3.6*	20.0 ± 3.9*	15.4 ± 3.4*
G4-PDRN+ESWT	5.3 ± 2.7*†‡	11.8 ± 2.9*†‡	9.3 ± 2.7*†‡
G5-ESWT+PDRN	9.8 ± 4.7*†‡	13.7 ± 3.3*†‡	12.3 ± 3.2*†‡

Values are presented as mean ± standard deviation; G1-Control: IC for 2 weeks and 0.2 ml of normal saline injection for 2 weeks after CR; G2-PDRN: IC for 2 weeks and 0.2 ml of PDRN injection for 2 weeks after CR; G3-ESWT: IC for 2 weeks and ESWT after CR; G4-PDRN+ESWT: IC for 2 weeks, 0.2 ml of PDRN injection and ESWT for 2 weeks after CR; G5-ESWT+PDRN: IC for 2 weeks, ESWT, and 0.2 ml of PDRN injection; IC: immobilized by cast; CR: cast removal; PDRN: polydeoxyribonucleotide; ESW: extracorporeal shock wave therapy. *) $p < 0.05$ one-way ANOVA, Tukey's post hoc test between group 1 and groups 2, 3, 4, and 5. †) $p < 0.05$ one-way ANOVA, Tukey's post hoc test between group 2 and groups 4 and 5. ‡) $p < 0.05$ one-way ANOVA, Tukey's post hoc test between group 3 and groups 4 and 5.

Table 2. Comparison of immunohistochemical findings in gastrocnemius muscle fiber among the five groups.

	G1-Control	**G2-PDRN**	**G3-ESWT**	**G4-PDRN+ESWT**	**G5-ESWT+PDRN**
Medial GCM					
Type I fiber CSA (μm²)	287.6 ± 5.5	469.4 ± 12.5*	716.8 ± 18.9*	1,391.9 ± 23.6*†‡	1,137.9 ± 21.1*†‡
Type II fiber CSA (μm²)	443.1 ± 4.5	1554.4 ± 21.4*	1,735.3 ± 26.2*	2,458.0 ± 50.6*†‡	2,046.6 ± 33.8*†‡
Total muscle fiber CSA (μm²)	399.0 ± 20.5	1394.0 ± 22.6*	1,542.2 ± 25.6*	2,162.0 ± 42.0*†‡	1,910.2 ± 31.5*†‡
VEGF ratio	0.15 ± 0.07	0.27 ± 0.02*	0.32 ± 0.02*	0.59 ± 0.03*†‡§	0.44 ± 0.03*†‡
PECAM-1 ratio	0.08 ± 0.05	0.21 ± 0.02*	0.28 ± 0.02*	0.59 ± 0.04*†‡§	0.42 ± 0.10*†‡
Lateral GCM					
Type I fiber CSA (μm²)	286.2 ± 12.3	446.8 ± 15.3*	697.9 ± 16.2*	1,441.2 ± 25.9*†‡	1,095.1 ± 22.0*†‡
Type II fiber CSA (μm²)	420.1 ± 4.9	1450.6 ± 20.3*	1607.1 ± 17.6*	2,460.4 ± 47.3*†‡	1,980.9 ± 27.6*†‡
Total muscle fiber CSA (μm²)	400.73 ± 4.8	1366.6 ± 20.7*	1,481.2 ± 18.5*	2,173.5 ± 40.0*†‡	1,858.5 ± 26.4*†‡
VEGF ratio	0.15 ± 0.05	0.29 ± 0.02*	0.35 ± 0.04*	0.57 ± 0.02*†‡§	0.47 ± 0.02*†‡
PECAM-1 ratio	0.08 ± 0.06	0.28 ± 0.02*	0.29 ± 0.04*	0.58 ± 0.02*†‡§	0.44 ± 0.03*†‡

Values are presented as mean ± standard deviation; G1-Control: IC for 2 weeks and 0.2 ml of normal saline injection for 2 weeks after CR; G2-PDRN: IC for 2 weeks and 0.2 ml of PDRN injection for 2 weeks after CR; G3-

 doi:10.20944/preprints202307.1799.v1

ESWT: IC for 2 weeks and ESWT after CR; G4-PDRN+ESWT: IC for 2 weeks, 0.2 ml of PDRN injection, and ESWT for 2 weeks after CR; G5-ESWT+PDRN: IC for 2 weeks, ESWT, and 0.2 ml of PDRN injection; IC: immobilized by cast; CR: cast removal; PDRN: polydeoxyribonucleotide; ESWT: extracorporeal shock wave therapy. *) $p < 0.05$ one-way ANOVA, Tukey's post hoc test between group 1 and groups 2, 3, 4, and 5. †) $p < 0.05$ one-way ANOVA, Tukey's post hoc test between group 2 and groups 4 and 5. ‡) $p < 0.05$ one-way ANOVA, Tukey's post hoc test between group 3 and groups 4 and 5. §) $p < 0.05$ one-way ANOVA, Tukey's post hoc test among group 4 and groups 1, 2, 3, and 5.

The VEGF and PECAM-1 ratios of the two GCM muscle fibers were significantly higher in Group 4 compared to the others ($p < 0.05$, Table 2, Figure 4). The VEGF ratios were significantly greater in Group 2 (PDRN) (0.27 ± 0.02 and 0.29 ± 0.02, respectively) and Group 3 (ESWT) (0.32 ± 0.02 and 0.35 ± 0.04, respectively) compared to Group 1 (normal saline) (0.17 ± 0.07 and 0.15 ± 0.05, respectively) ($p < 0.05$, Table 2, Figure 4). Similarly, the PECAM-1 ratios of the medial and lateral GCM muscle fibers were significantly higher in Group 2 (0.21 ± 0.02 and 0.28 ± 0.02, respectively) and Group 3 (0.28 ± 0.02 and 0.29 ± 0.04, respectively) compared to Group 1 (0.08 ± 0.05 and 0.08 ± 0.06, respectively) ($p < 0.05$, Table 2, Figure 4). The VEGF and PECAM-1 ratios between Groups 2 and 3 did not differ significantly (Table 2).

The densities of PECAM-1, PCNA, and VEGF expression were significantly increased in Group 4 (PDRN+ESWT) and Group 5 (ESWT+PDRN) compared to Group 1 (normal saline), Group 2 (PDRN), and Group 3 (ESWT) ($p < 0.05$, Table 3, Figure 5). The densities of PECAM-1 were 1.19 ± 0.11, 1.32 ± 0.09, 1.72 ± 0.08, and 1.77 ± 0.09, the densities of PCNA were 1.30 ± 0.08, 1.50 ± 0.12, 1.85 ± 0.13, and 1.86 ± 0.11, and the densities of VEGF were 1.38 ± 0.13, 1.60 ± 0.07, 1.90 ± 0.07, and 1.88 ± 0.12 in Group 2 (PDRN), Group 3 (ESWT), Group 4 (PDRN+ESWT), and Group 5 (ESWT+PDRN), respectively, when Group 1 (normal saline) was considered as 1.

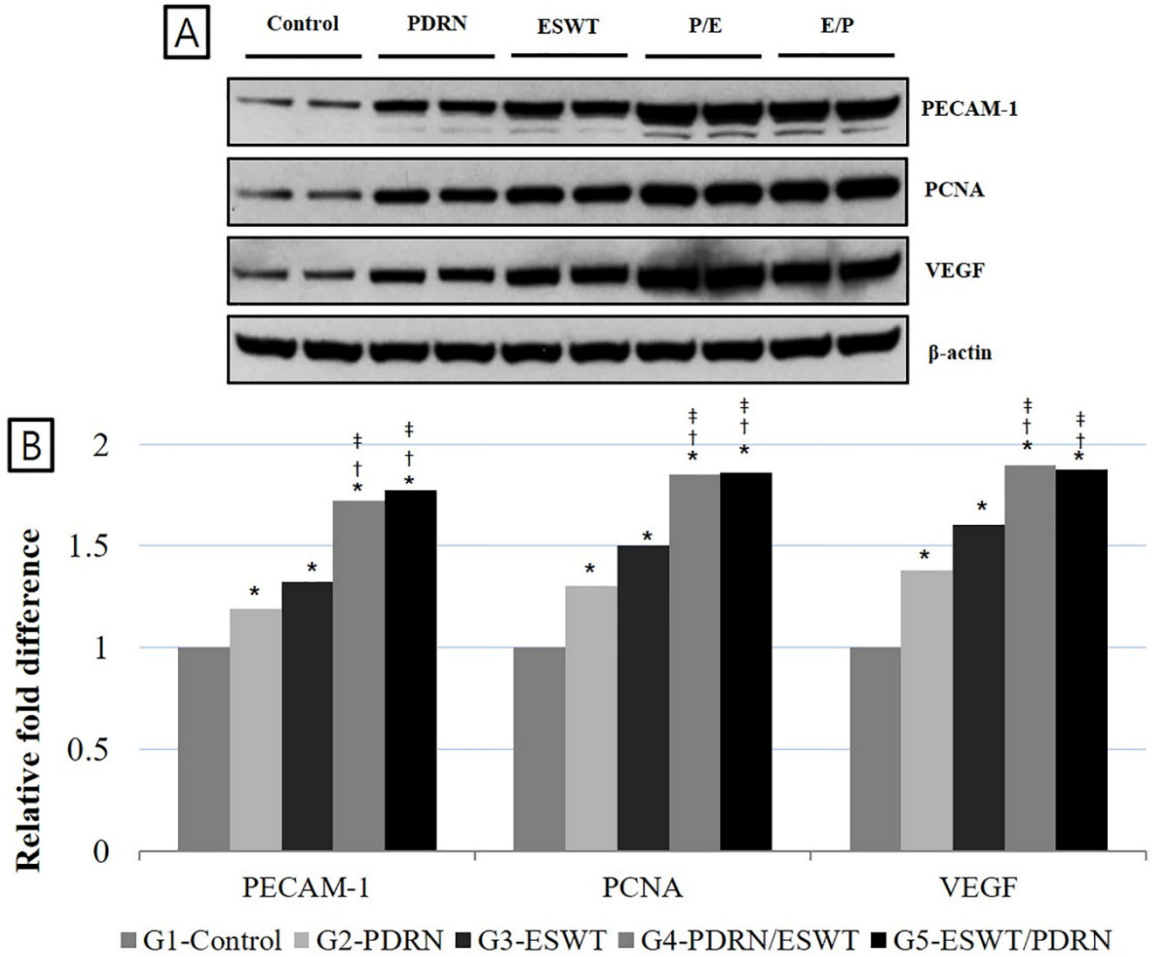

Preprints (www.preprints.org) | NOT PEER-REVIEWED | Posted: 26 July 2023 doi:10.20944/preprints202307.1799.v1

Figure 5. Expression of PECAM-1, PCNA, and VEGF proteins in the medial GCM muscle fibers among the five groups (A) Protein levels of PECAM-1, PCNA, and VEGF. A representative western blot is shown. (B) A relative density (% Control) among the five groups is presented. *) $p < 0.05$ one-way ANOVA, Tukey's post hoc test between group 1 and groups 2, 3, 4, and 5. †) $p < 0.05$ one-way ANOVA, Tukey's post hoc test between group 2 and groups 4 and 5. ‡) $p < 0.05$ one-way ANOVA, Tukey's post hoc test between group 3 and groups 4 and 5. VEGF: vascular endothelial growth factor; PECAM-1: platelet endothelial cell adhesion molecule-1; GCM: gastrocnemius; NS: normal saline; PDRN: polydeoxyribonucleotide; ESWT: extracorporeal shock wave therapy; ANOVA: analysis of variance.

Table 3. Comparison of Western blot findings in gastrocnemius muscle fiber among the five groups.

	G1-Control	G2-PDRN	G3-ESWT	G4-PDRN+ESWT	G5-ESWT+PDRN
Relative fold differences					
PECAM-1	1	1.19 ± 0.11*	1.32 ± 0.09*	1.72 ± 0.08*†‡	1.77 ± 0.09*†‡
PCNA	1	1.30 ± 0.08*	1.50 ± 0.12*	1.85 ± 0.13*†‡	1.86 ± 0.11*†‡
VEGF	1	1.38 ± 0.13*	1.60 ± 0.07*	1.90 ± 0.07*†‡	1.88 ± 0.12*†‡

Values are presented as mean ± standard deviation. G1-Control: IC for 2 weeks and 0.2 ml of normal saline injection for 2 weeks after CR; G2-PDRN: IC for 2 weeks and 0.2 ml of PDRN injection for 2 weeks after CR; G3-ESWT: IC for 2 weeks and ESWT after CR; G4-PDRN+ESWT: IC for 2 weeks, 0.2 ml of PDRN injection, and ESWT for 2 weeks after CR; G5-ESWT+PDRN: IC for 2 weeks, ESWT, and 0.2 ml of PDRN injection. VEGF: vascular endothelial growth factor; PECAM-1: platelet endothelial cell adhesion molecule-1; GCM: gastrocnemius; NS: normal saline; PDRN: polydeoxyribonucleotide; ESWT: extracorporeal shock wave therapy; ANOVA: analysis of variance. *) $p < 0.05$ one-way ANOVA, Tukey's post hoc test between group 1 and groups 2, 3, 4, and 5. †) $p < 0.05$ one-way ANOVA, Tukey's post hoc test between group 2 and groups 4 and 5. ‡) $p < 0.05$ one-way ANOVA, Tukey's post hoc test between group 3 and groups 4 and 5.

4. Discussion

In our study, we aimed to investigate the synergistic effects of PDRN injection and ESWT on atrophied calf muscles in a cast-immobilized rabbit model. Our findings revealed that the combination of PDRN injection and ESWT was superior in promoting muscle regeneration compared to PDRN injection alone or ESWT alone. The atrophic changes in the gastrocnemius muscle were significantly reduced in the groups that received the combined treatment compared to the other groups. Notably, the timing of ESWT application in relation to PDRN injection also influenced the outcomes, with improved results observed when ESWT was applied after PDRN injection. From a clinical perspective, ESWT has proven to be an effective therapeutic approach for the indicated musculoskeletal conditions [10,11,18,19]. In our study, we utilized radial ESWT to treat atrophy of muscles in rabbits. The radial type of ESWT offers certain advantages compared to the focused type. It has less surface infiltration and distributes energy more evenly across the treatment area [20]. Recent systematic reviews have highlighted the benefits of radial ESWT, including a larger coverage area for therapy, reduced requirement for precise targeting, and elimination of the need for additional local anesthesia [21]. Considering that our animal model exhibited overall atrophy of the gastrocnemius (GCM) muscle, we specifically selected radial ESWT for this study instead of the focused type.

No former studies have directly explored the application of ESWT for the treatment of atrophied muscles. However, there is one study that utilized ESWT for the management of myofascial pain syndrome (MPS) [22]. In their research, they administered 1500 pulses of ESWT once a week for 2 weeks, following a similar protocol to our current study. Their results demonstrated significant improvements in pain relief and subjective disability among MPS patients [22].

The primary purpose of the study was to evaluate the potential of ESWT in promoting the rehabilitation from muscle atrophy induced by immobilization. Shock waves, which are sound waves with high positive pressure amplitudes, possess unique characteristics compared to ultrasonic waves with limited bandwidth. These high-pressure sound waves exhibit increased velocity and generate significant energy by modifying their waveform. Although the process of ESWT is still a subject of

 doi:10.20944/preprints202307.1799.v1

debate, previous studies have suggested that it may promote angiogenesis [23] and tenocyte proliferation [24], which could contribute to pain reduction and facilitate functional recovery. Zhang et al. proposed that ESWT is involved in lubricin production in tendons and septa, offering a potential mechanism for reducing tissue wear and tear [25]. In addition, a laboratory study demonstrated that radial ESWT significantly upregulated the expression of muscle-specific genes, including paired box protein 7 (Pax7), neural cell adhesion molecule, and myogenic factor 5 (Myf5), in muscle cells compared to non-treated cells [26].

In our study, we observed significant improvements in various parameters related to muscle regeneration, including calf muscle circumference, GCM muscle thickness, tibial nerve CMAP, and GCM muscle fiber CSA (type I, II, and total) in the G4-PDRN+ESWT and G5-ESWT+PDRN groups compared to the other groups. These results are comparable to those of the previous studies that have reported the enhanced expression of tissue-specific growth factors following short-term post-injury ESWT [8,9,15,23,24].

Experimental studies conducted in animal models involving injured bones, tendons, and toxin-lesioned limb muscles have also demonstrated similar responses to ESWT [15,24,27–29]. These studies have revealed that ESWT induces the upregulation of factors such as VEGF, VEGF receptor protein, placental growth factor (PGF), PGF receptor, and transforming growth factor β1, thereby promoting angiogenesis and tissue healing [30]. We observed a significantly higher VEGF and PECAM-1 (platelet endothelial cell adhesion molecule-1) ratio in the GCM muscle fibers of the G4-PDRN+ESWT group compared to the other four groups. This finding is in line with the study by Frey et al., which detected remarkable repair of injured muscle in a locally VEGF-treated rabbit group, attributed to reduced connective tissue and increased muscle fiber count [31]. PECAM-1, known for its involvement in angiogenesis, plays an essential role in the healing and regenerative processes [31,32].

Our findings suggest that PDRN injection may be beneficial in promoting the recovery of muscle atrophy caused by immobilization. Previous research has demonstrated that PDRN has the ability to promote cell growth and migration, stimulate the production of extracellular matrix proteins, and reduce inflammation [33,34]. PDRN can also enter cells and provide pyrimidine or purine rings, serving as substrates for enzymes involved in nucleic acid production [35]. Purine nucleosides, derived from PDRN, can activate various signaling pathways by binding to specific receptors, activating reproduction of endothelial cells and neuroglia [36], and displaying synergistic effects with other growth factors [37–39]. Studies have shown that PDRN promotes the expression of VEGF by activating the adenosine A2A receptor [33]. Moreover, recent research has demonstrated that VEGF promotes healing in diabetic rat feet by inducing angiogenesis and collagen synthesis [35]. Therefore, PDRN may enhance the healing process in atrophied muscles that often exhibit poor vascularization [1,2]. According to our results, we suppose that ESWT-induced VEGF expression enhances the regenerative effects of PDRN, as evidenced by a significantly higher VEGF and PECAM-1 ratio observed in the G4-PDRN+ESWT group compared to the other groups.

The precise mechanism underlying the joint effects of ESWT and PDRN are not yet fully understood. However, this mode may provide advantages due to the localized property of ESWT-induced cavitation and its potential impact on endothelial cell membranes [40]. Cavitation refers to the formation of bubbles with conflicting pressures, which can exert stress on cell membranes. This "shearing stress" can increase cell membrane permeability and induce gene expression by activating growth factors [41]. Further research is required to reveal the precise mechanisms of synergistic effects of ESWT and PDRN in facilitating muscle regeneration and tissue healing.

A previous study [42] did not observe an improved effect of the combined treatment with cisplatin before or after shock wave treatment. The authors proposed that this result may be attributed to the short-lived effect of ESWT, lasting approximately 15 seconds after the last shock wave, and the permeable nature of cell membranes [43]. However, in contrast, another study indicated that ESWT enhanced anesthesia of rat caudal nerve, showing the potential possibility of shock wave-mediated transdermal drug delivery during the ESWT period [44]. The group receiving EMLA combined with ESWT possessed greater anesthetic capabilities compared to the group

applying EMLA after ESWT. These findings are consistent with our study, indicating a synergistic regenerative effect. Our results demonstrate superior effects in certain aspects when ESWT is applied after PDRN injection.

However, our study has several limitations. Firstly, the evaluation period was limited to 4 weeks, including baseline, 2 weeks of immobilization, and PDRN injections. Therefore, the long-term effects of PDRN injections, with or without ESWT, on atrophied muscles should be further investigated. Secondly, we conducted two sessions of ESWT using a radial-type machine with specific parameters, including a frequency of 3 Hz, energy density of 0.1 mJ/mm2, and 1500 pulses per session. The potential differences in the efficacy of ESWT at varying physical characteristics were not evaluated in our study. Future studies should explore more appropriate interventions for atrophied muscles.

This study investigated the effectiveness of combining ESWT with PDRN injection in the treatment of atrophy in rabbit models. The results demonstrated that the combined intervention was more effective than ESWT alone, PDRN injection alone, or injection with normal saline. The mechanism of action involved the upregulation of VEGF and PECAM-1, which are associated with angiogenesis. The combined treatment also led to improvements in calf circumference, gastrocnemius muscle thickness, tibial nerve compound muscle action potential (CMAP), and gastrocnemius muscle fiber CSA. Interestingly, applying ESWT after PDRN injection showed superior effects in promoting angiogenesis compared to applying ESWT before PDRN injection. These findings suggest that the sequential application of ESWT after PDRN injection may enhance the outcomes of conservative treatments for atrophied muscles.

Authors' contributions:(I) Conception and design: *K.D.R, L.Y.J,* (II) Administrative support: *K.D.R,* (III) Provision of study materials or patients: *K.D.R,* (IV) Collection and assembly of data: *K.D.R, M.Y.S, L.Y.J, and C.S.C,* (V) Data analysis and interpretation: All authors., (VI) Manuscript writing: All authors., (VII) Final approval of manuscript: All authors.

Funding: The authors disclosed receipt of the following financial support for the research, authorship, and/or publication of this article: This work was supported by the Basic Science Research Program through the National Research Foundation of Korea (NRF) funded by the Ministry of Education, Science, and Technology (MEST) (2022R1A2C2091162).

Data Sharing Statement: All data generated or analyzed during this study are included in this published article.

Conflicts of Interest: All authors have completed the ICMJE uniform disclosure form. All authors have no conflicts of interest to declare.

Ethical statement: The authors are accountable for all aspects of the work in ensuring that questions related to the accuracy or integrity of any part of the work are appropriately investigated and resolved. The study was conducted according to the guidelines of the IACUC, and approved by the Catholic University of Daegu School of Medicine Animal Care and Use Committee.

Footnote: *Reporting Checklist:* The authors have completed the ARRIVE reporting checklist.

Abbreviations

PDRN = polydeoxyribonucleotide, VEGF = vascular endothelial growth factor, ESWT = extracorporeal shock wave therapy, IC = immobilization by cast, GCM = gastrocnemius, CMAP = complex muscle action potential, PBS = phosphate-buffered saline, CSA = cross-sectional area, *PECAM*-1 = platelet endothelial cell adhesion molecule-1.

References

1. Fujino H, Kohzuki H, Takeda I, Kiyooka T, Miyasaka T, Mohri S, et al. Regression of capillary network in atrophied soleus muscle induced by hindlimb unweighting. *J Appl Physiol (1985).* **2005,** *98,* 1407–1413.
2. Dirks ML, Wall BT, Snijders T, Ottenbros CL, Verdijk LB, van Loon LJ. Neuromuscular electrical stimulation prevents muscle disuse atrophy during leg immobilization in humans. *Acta Physiol (Oxf).* **2014,** *210,* 628–641.
3. Bergouignan A, Rudwill F, Simon C, Blanc S. Physical inactivity as the culprit of metabolic inflexibility: evidence from bed-rest studies. *J Appl Physiol (1985).* **2011**, *111*, 1201–1210.

4. Kim JK, Chung JY. Effectiveness of polydeoxyribonucleotide injection versus normal saline injection for treatment of chronic plantar fasciitis: a prospective randomised clinical trial. *Int Orthop.* **2015**, *39*, 1329–1334.
5. Bitto A, Polito F, Irrera N, D'Ascola A, Avenoso A, Nastasi G, et al. Polydeoxyribonucleotide reduces cytokine production and the severity of collagen-induced arthritis by stimulation of adenosine A($_2$A) receptor. *Arthritis Rheum*. **2011**, *63*, 3364–3371.
6. Bitto A, Galeano M, Squadrito F, Minutoli L, Polito F, Dye JF, et al. Polydeoxyribonucleotide improves angiogenesis and wound healing in experimental thermal injury. *Crit Care Med*. **2008**, *36*, 1594–1602.
7. Galeano M, Bitto A, Altavilla D, Minutoli L, Polito F, Calò M, et al. Polydeoxyribonucleotide stimulates angiogenesis and wound healing in the genetically diabetic mouse. *Wound Repair Regen*. **2008,** *16*, 208–217.
8. Assaly R, Giuliano F, Clement P, Laurin M, Favier M, Teo P, et al. Extracorporeal shock waves therapy delivered by aries improves erectile dysfunction in spontaneously hypertensive rats through penile tissue remodeling and neovascularization. *Sex Med*. **2019**, *7*, 441–450.
9. Murata R, Ohtori S, Ochiai N, Takahashi N, Saisu T, Moriya H, et al. Extracorporeal shockwaves induce the expression of ATF3 and GAP-43 in rat dorsal root ganglion neurons. *Auton Neurosci*. **2006**, *128*, 96–100.
10. Rompe JD, Decking J, Schoellner C, Nafe B. Shock wave application for chronic plantar fasciitis in running athletes. A prospective, randomized, placebo-controlled trial. *Am J Sports Med*. **2003**, *31*, 268–275.
11. Spacca G, Necozione S, Cacchio A. Radial shock wave therapy for lateral epicondylitis: a prospective randomised controlled single-blind study. *Eura Medicophys*. **2005**, *41*, 17–25.
12. Martínez IM, Sempere-Rubio N, Navarro O, Faubel R. Effectiveness of shock wave therapy as a treatment for spasticity: A systematic review. *Brain Sci*. **2020**, *11*, 15.
13. Hsu PC, Chang KV, Chiu YH, Wu WT, Özçakar L. Comparative effectiveness of botulinum toxin injections and extracorporeal shockwave therapy for post-stroke spasticity: A systematic review and network meta-analysis. *EClinicalmedicine*. **2022**, *43*, 101222.
14. Lee JH, Cho SH. Effect of extracorporeal shock wave therapy on denervation atrophy and function caused by sciatic nerve injury. *J Phys Ther Sci*. **2013**, *25*, 1067–1069.
15. Zissler A, Steinbacher P, Zimmermann R, Pittner S, Stoiber W, Bathke AC, et al. Extracorporeal shock wave therapy accelerates regeneration after acute skeletal muscle injury. *Am J Sports Med*. **2017,** *45*, 676–684.
16. Kim DH, Kwon DR, Park GY, Moon YS. Synergetic effects of shock waves with polydeoxyribonucleotides on rotator cuff tendon tear in a rabbit model. *Biocell*. **2021,** *45*, 527-536.
17. Kauhanen S, von Boguslawsky K, Michelsson JE, Leivo I. Satellite cell proliferation in rabbit hindlimb muscle following immobilization and remobilization: an immunohistochemical study using MIB 1 antibody. *Acta Neuropathol*. **1998**, *95*, 165–170.
18. Schmitz C, Császár NB, Milz S, Schieker M, Maffulli N, Rompe JD, et al. Efficacy and safety of extracorporeal shock wave therapy for orthopedic conditions: a systematic review on studies listed in the PEDro database. *Br Med Bull*. **2015,** *116*, 115–138.
19. Park DS, Kwon DR, Park GY, Lee MY. Therapeutic effect of extracorporeal shock wave therapy according to treatment session on gastrocnemius muscle spasticity in children with spastic cerebral palsy: A pilot study. *Ann Rehabil Med*. **2015**, *39*, 914–921.
20. Wu YT, Ke MJ, Chou YC, Chang CY, Lin CY, Li TY, et al. Effect of radial shock wave therapy for carpal tunnel syndrome: A prospective randomized, double-blind, placebo-controlled trial. *J Orthop Res*. **2016**, *34*, 977–984.
21. Chang KV, Chen SY, Chen WS, Tu YK, Chien KL. Comparative effectiveness of focused shock wave therapy of different intensity levels and radial shock wave therapy for treating plantar fasciitis: a systematic review and network meta-analysis. *Arch Phys Med Rehabil.* **2012,** *93*, 1259–1268.
22. Park KD, Lee WY, Park MH, Ahn JK, Park Y. High- versus low-energy extracorporeal shock-wave therapy for myofascial pain syndrome of upper trapezius: A prospective randomized single blinded pilot study. *Med (Baltim)*. **2018**, *97*, e11432.
23. Wang CJ, Huang HY, Pai CH. Shock wave-enhanced neovascularization at the tendon-bone junction: an experiment in dogs. *J Foot Ankle Surg*. **2002**, *41*, 16–22.
24. Chen YJ, Wang CJ, Yang KD, Kuo YR, Huang HC, Huang YT, et al. Extracorporeal shock waves promote healing of collagenase-induced Achilles tendinitis and increase TGF-beta1 and IGF-I expression. *J Orthop Res*. **2004**, *22*, 854–861.
25. Zhang D, Kearney CJ, Cheriyan T, Schmid TM, Spector M. Extracorporeal shockwave-induced expression of lubricin in tendons and septa. *Cell Tissue Res*. **2011**, **346**, 255-262.
26. Mattyasovszky SG, Langendorf EK, Ritz U, Schmitz C, Schmidtmann I, Nowak TE, et al. Exposure to radial extracorporeal shock waves modulates viability and gene expression of human skeletal muscle cells: a controlled in vitro study. *J Orthop Surg Res*. **2018**, *13*, 75.
27. Holfeld J, Tepeköylü C, Blunder S, Lobenwein D, Kirchmair E, Dietl M, et al. Low energy shock wave therapy induces angiogenesis in acute hind-limb ischemia via VEGF receptor 2 phosphorylation. *PLOS ONE*. **2014**, *9*, e103982.

28. Wang CJ, Wang FS, Yang KD. Biological effects of extracorporeal shockwave in bone healing: a study in rabbits. *Arch Orthop Trauma Surg*. **2008**, *128*, 879–884.
29. Barnes K, Lanz O, Werre S, Clapp K, Gilley R. Comparison of autogenous cancellous bone grafting and extracorporeal shock wave therapy on osteotomy healing in the tibial tuberosity advancement procedure in dogs. Radiographic densitometric evaluation. *Vet Comp Orthop Traumatol*. **2015**, *28*, 207–214.
30. Frey SP, Jansen H, Raschke MJ, Meffert RH, Ochman S. VEGF improves skeletal muscle regeneration after acute trauma and reconstruction of the limb in a rabbit model. *Clin Orthop Relat Res*. **2012**, *470*, 3607–3614.
31. DeLisser HM, Christofidou-Solomidou M, Strieter RM, Burdick MD, Robinson CS, Wexler RS, et al. Involvement of endothelial PECAM-1/CD31 in angiogenesis. *Am J Pathol*. **1997**, *151*, 671–677.
32. DiPietro LA. Angiogenesis and wound repair: when enough is enough. *J Leukoc Biol*. **2016**, *100*, 979–984.
33. Veronesi F, Dallari D, Sabbioni G, Carubbi C, Martini L, Fini M. Polydeoxyribonucleotides (PDRNs) from skin to musculoskeletal tissue regeneration via adenosine A(2A) receptor involvement. *J Cell Physiol*. **2017**, *232*, 2299–2307.
34. Kim JK, Chung JY. Effectiveness of polydeoxyribonucleotide injection versus normal saline injection for treatment of chronic plantar fasciitis: a prospective randomised clinical trial. *Int Orthop*. **2015**, *39*, 1329–1334.
35. Altavilla D, Bitto A, Polito F, Marini H, Minutoli L, Di Stefano V, et al. Polydeoxyribonucleotide (PDRN): a safe approach to induce therapeutic angiogenesis in peripheral artery occlusive disease and in diabetic foot ulcers. *Cardiovasc Hematol Agents Med Chem*. **2009**, *7*, 313–321.
36. Rathbone MP, Middlemiss PJ, Gysbers JW, DeForge S, Costello P, Del Maestro RF. Purine nucleosides and nucleotides stimulate proliferation of a wide range of cell types. *In Vitro Cell Dev Biol*. **1992**, 28A, 529–536.
37. Rathbone MP, Deforge S, Deluca B, Gabel B, Laurenssen C, Middlemiss P, et al. Purinergic stimulation of cell division and differentiation: mechanisms and pharmacological implications. *Med Hypotheses*. **1992**, *37*, 213–219.
38. Wang DJ, Huang NN, Heppel LA. Extracellular ATP shows synergistic enhancement of DNA synthesis when combined with agents that are active in wound healing or as neurotransmitters. *Biochem Biophys Res Commun*. **1990**, 166, 251–258.
39. Kwon DR, Park GY, Lee SC. Treatment of full-thickness rotator cuff tendon tear using umbilical cord blood-derived mesenchymal stem cells and polydeoxyribonucleotides in a rabbit model. *Stem Cells Int*. **2018**, *2018*, 7146384.
40. Notarnicola A, Moretti B. The biological effects of extracorporeal shock wave therapy (eswt) on tendon tissue. *Muscles Ligaments Tendons J*. **2012**, *2*, 33–37.
41. Apfel RE. Acoustic cavitation: a possible consequence of biomedical uses of ultrasound. *Br J Cancer Suppl*. **1982**, *5*, 140–146.
42. Gambihler S, Delius M. In vitro interaction of lithotripter shock waves and cytotoxic drugs. *Br J Cancer*. **1992**, *66*, 69–73.
43. López-Marín LM, Rivera AL, Fernández F, Loske AM. Shock wave-induced permeabilization of mammalian cells. *Phys Life Rev*. **2018**, *26–27*, 1–38.
44. Luh JJ, Huang WT, Lin KH, Huang YY, Kuo PL, Chen WS. Effects of extracorporeal shock wave-mediated transdermal local anesthetic drug delivery on rat caudal nerves. *Ultrasound Med Biol*. **2018**, *44*, 214–222.